An Acad Bras Cienc (2022) 94(Suppl. 4): e20200797 DOI 10.1590/0001-3765202220200797
Anais da Academia Brasileira de Ciências | *Annals of the Brazilian Academy of Sciences*
Printed ISSN 0001-3765 I Online ISSN 1678-2690
www.scielo.br/aabc | www.fb.com/aabcjournal

GEOSCIENCES

South Atlantic explosive cyclones in 2014-2015: study employing NCEP2 and MERRA-2 reanalyses

HUGO N. ANDRADE, ANDRÉ B. NUNES & MATEUS S. TEIXEIRA

Abstract: An analysis of explosive cyclone cases was produced by comparing the reanalysis of MERRA-2 (high spatial resolution) and NCEP2 (low spatial resolution) to South Atlantic in the 2014-2015 period. A total of 51 cases were found, of which 49 were detected by the first reanalysis and 33 by the second (2 cases identified by NCEP2 were not identified by MERRA-2). Spring was the dominant season in the formation of the cases in both reanalyses. It was observed that most systems are formed preferentially eastward of a preexisting trough at higher levels, while others are formed under an almost zonal upper airstream. This difference is more evident in the NCEP2. It was also diagnosed that the MERRA-2 shows more clearly the diffluence in the 250 hPa flow. The analysis of the composite fields revealed a negative horizontal tilt of the trough in 500 hPa, influenced by intense convection as the system develops. Besides, it pointed to a more pronounced jet stream in intense explosive cyclones and more prominent diffluence in non-intense cases. Since the NCEP2 reanalysis detected fewer cases (and only 2 intense) than MERRA-2, it was considered that the former is less suited to the analysis of this type of event.

Key words: Bombogenesis, composite fields, diffluent flow, extratropical cyclone.

INTRODUCTION

The climate of southern South America is strongly influenced by the frequent occurrence of extratropical cyclones - low-pressure transient systems on a synoptic scale, featuring cyclonic geostrophic vorticity. Its formation period is called cyclogenesis. In large part, mid-latitude cyclogenesis observed in the low troposphere occurs combined with the surface frontal zone. Along with this, there is a wave at upper levels that plays an important role in the generation and conversion of energy and the cyclonic vorticity advection as well (Kousky & Elias 1982, Wash et al. 1992, Lim & Simmonds 2002, Vera et al. 2002, Dias Pinto & Da Rocha 2011, Avila et al. 2016). Advection of temperature at low levels indicates the role of air masses in the development of the cyclone, amplifying the upper troposphere wave. Such features are expected in transient systems with a strong meridional temperature gradient, that is, baroclinic instabilities (Bluestein 1993). Besides that, diabatic processes like latent and sensible heat fluxes, are also important mechanisms for extratropical cyclones formation (Atlas 1987, Seluchi & Saulo 1988, Piva 2001, Piva et al. 2008, Schultz et al. 2018). In the last few decades, several studies have addressed the behavior of cyclones in South America, especially those that developed on the Atlantic Ocean. Satyamurty et al. (1990), through satellite images between 1980-1986, identified a higher frequency of extratropical cyclones in the summer and less in the winter, indicating the importance of thermal factors on the formation of the systems. On the other hand, through surface charts between 1979-1988, Gan & Rao

(1991) found greater frequency in the winter and identified two most favorable regions for cyclogenesis: one around Uruguay and another near to Gulf of San Matias in Argentina. Sinclair (1994, 1995) show the east coast of South America as favorable to cyclogenesis, including those of rapid development, with greater frequency in winter and trajectories to east and south, as well as Gan & Rao (1991). Andes Cordillera has an important role in lee cyclogenesis, as presented, for example, in Gan & Rao (1994) and Hoskins & Hodges (2005). Reboita et al. (2010), through RegCM3 simulations, identified the cyclogenetic areas pointed out in Gan & Rao (1991), in addition to a third one, featuring less intense systems, on the coast of south-southeastern Brazil.

Cyclogenesis can also be classified according to its intensity, determined from the increment of cyclonic vorticity associated with the cyclone or, more usually, from the drop in the cyclone's central pressure (Gan & Seluchi, 2009). According to Sanders & Gyakum (1980), cyclones called explosives, or "bombs", are characterized by a decrease of at least 1 hPa/h in 24 hours to the reference latitude of 60º. The resulting critical rate, denoted by 1 Bergeron (B), ranges from 28 hPa/24h at the pole and 12 hPa/24h at the latitude of 25º. These systems are formed preferably over the ocean, where surface heat fluxes are important in preparing the environment for the explosive phase (Piva et al. 2011). They are also generated in regions where there is strong baroclinicity with intense horizontal temperature gradients at the surface (Sanders & Gyakum 1980, Roebber 1984), producing strong winds, low visibility, large amounts of precipitation, and dangerous ocean conditions as a result of this rapid change in central pressure (Allen et al. 2010). Thus, explosive cyclones have a potential for socio-economic impact greater than ordinary cyclones, especially in coastal regions.

Increasingly, reanalysis datasets have been a great tool in investigating atmospheric systems. Reanalysis data are a strategy to fill gaps in the observation system and diagnose variables that are unable to be measured directly (Kennedy et al. 2011). Since each reanalysis uses different models and data assimilation systems, the methodologies applied lead to a distinct view of the atmosphere in the final products. Therefore, it is interesting to compare different products and analyze any discrepancies and their causes – what justifies a large number of papers using different sources of reanalysis data (Hodges et al. 2003, Bengtsson et al. 2004, Mendes et al. 2009, Kennedy et al. 2011, Hodges et al. 2011, 2017, Kuwano-Yoshida & Enomoto 2013, Pillar et al. 2018, for example).

In a climatology of cyclones made for the North Atlantic, Hanson et al. (2004) compared the reanalysis from ECMWF, ERA-15 (which was extended from 1994 to 2001 using operational analyses in the same way as Hoskins & Hodges (2002)), with the NCEP/NCAR reanalysis and showed that the data of the first (higher resolution) produced a more comprehensive climatology of the studied region at all scales. Trigo (2006) made a climatology of storm-tracks in the European Atlantic sector, also observing their annual variability, comparing the reanalyses ERA-40 and NCEP/NCAR. The author showed a strong discrepancy in the number of storms in each dataset (higher for ERA-40) resulting from differences in the resolution of the fields due to the detection algorithm and also from the models' integration features and assimilation schemes used in each reanalysis. Despite the differences in the number of events, both reanalyses agreed on the main areas of storm-track activity. Allen et al. (2010), comparing multiple reanalyses for a global climatology of explosive cyclones, showed a preferred region of formation, with the maximum for the Southern

Hemisphere between 30°S and 50°S, 70°W and 10°W, more specifically in the cyclogenetic region identified by Gan & Rao (1991) and Reboita et al. (2010), on the southeast coast of the South American continent. The authors indicated winter as the most frequent season of these systems, a characteristic found in Bitencourt et al. (2013) as well, and also showed that high resolution and modern reanalyses increase the density of rapidly intensifying cyclones, agreeing with the other authors mentioned above.

Relatively, few authors have focused their studies on comparisons between reanalyses for the Southern Hemisphere, especially for explosive cyclones. Since these datasets are always being updated, this study aims to show a comparison between the analyses of explosive cyclone cases that occurred in the South Atlantic in 2014 and 2015, using reanalyses of very different spatial resolutions (MERRA-2 and NCEP2, described below), pointing out dynamic and synoptic aspects related to these events.

MATERIALS AND METHODS

Reanalysis data

The following data were used: mean sea level pressure (mslp), geopotential height at 500 hPa, and wind components u and v at 250 hPa from the Second Modern-Era Retrospective–Analysis for Research and Applications (MERRA-2) with 0,5º latitude and 0,66º longitude of spatial resolution and interpolations for 42 vertical levels (Bosilovich et al. 2016). These data were selected for the years 2014 and 2015, a period that collected a sufficient number of cases for this work's purpose and presented approximately neutral conditions concerning the El Niño Southern Oscillation (ENSO) phenomenon. This MERRA-2 dataset replaces the original MERRA reanalysis (Rienecker et al. 2011) using an updated version of the Goddard Earth Observing System Model, Version 5 (GEOS-5) data assimilation system, which allows larger data collections. Several works employing MERRA-2 data for different purposes are found in the American Meteorological Society Special Collection organized by Michael Bosilovich, available at (https://journals.ametsoc.org/topic/merra-2).

For comparison, data from the same variables and period were used from the reanalysis of the National Centers for Environmental Prediction – Department of Energy Atmospheric Model Intercomparison – II (NCEP2) with 2,5º latitude and 2,5º longitude of spatial resolution and 17 vertical levels (Kanamitsu et al. 2002), covering the same period obtained from MERRA-2. This dataset is an updated version of the first reanalysis NCEP/NCAR (Kalnay et al. 1996), with error correction from the previous one and use of an improved prediction model and data assimilation system, being recommended for transient systems analysis in the Southern Hemisphere (Kanamitsu et al. 2002). As well as MERRA-2, the NCEP2 dataset is also widely employed for different purposes, for example, climate modeling (Liang et al. 2004), analysis of teleconnections (Claud & Terray 2007), monsoons (Gu et al. 2010), monitoring of drought (Yao et al. 2010) and tropical cyclones (Choi et al. 2016).

Identification of explosive cyclones

All locations with trough and closed isobars on the surface, inside the spatial domain addressed in the study (15°S and 60°S, 75°W and 10°W), were visually identified in the mslp fields. Subsequently, the mslp values of the grid points referring to the centers of the closed isobars or troughs were obtained, to verify the existence and the exact position of the local minimum. Thus, it was possible to identify the beginning of the system, its trajectory, and the Normalized Deepening Rate (NDR), in Bergeron (B), during the development of the cyclone. According to Sanders & Gyakum (1980):

$$NDR = \frac{\Delta P}{24} * \frac{sen\ 60º}{sen\ \varphi}$$

being *ΔPc* the central pressure change in 24 hours and φ the average position related to the latitude, considering the start and end points of the system position during the explosive phase. When the result is greater than or equal to 1B, the system is considered to be rapidly developing, that is, an explosive cyclone.

Explosive cyclones were distinguished in intensity: 1,00 ≤ NDR < 1,30 are weak, 1,30 ≤ NDR ≤ 1,80 are moderate and NDR > 1,80 are intense. This intensity classification differs slightly from that proposed by Sanders (1986), which classifies weak explosive cyclones as 1,0 ≤ NDR ≤ 1,2 and moderate as 1,3 ≤ NDR ≤ 1,80. Since the present work considers two decimal places, weak and moderate classes were slightly modified, concerning Sanders (1986) definitions. As well as for intensity, the cases were distinguished according to Petterssen and Smebye (1971), that is, in type A (surface systems that form without the pre-existence of an upper-level trough) and type B (surface systems initiate downstream of a pre-existing upper-level trough) by visual analysis of upper-level fields and mslp.

From the minimum mslp values, composite fields centered on these values were generated, during the explosive phase, for the intense (NDR > 1,80) and non-intense (NDR ≤ 1,80) systems.

RESULTS AND DISCUSSION

Comparisons between reanalysis

Through MERRA-2 data (higher spatial resolution - 0,5° latitude × 0,66° longitude), 49 cases were found. Using data from NCEP2 (lower spatial resolution - 2,5° latitude × 2,5° longitude), 31 of these 49 cases were identified. There were 2 cases found using NCEP2 that were not observed through MERRA-2. Thus, a total of 51 cases were observed (Tables I and II). The difference in the number of detections using different spatial resolutions was also found in Gyakum et al. (1996), which showed that significant improvements in the detection of the central cyclone pressure occur as a consequence of an increase in horizontal resolution.

Regarding the seasonal distribution of the systems, in the MERRA-2 reanalysis the highest frequency was observed in the spring, followed by summer, then autumn and winter with the same number of cases. With the NCEP2 reanalysis, a similar result was observed, except autumn and winter frequencies were distinct (Table III).

The results mentioned above do not agree on frequency and seasonality with the climatology made by Bitencourt et al. (2013). Using data from NCEP/NCAR reanalysis, the authors used the cyclone identification method proposed by Murray & Simmonds (1991), classifying explosive cyclones in the cyclogenetic area of South America as rare phenomena, identifying, on average, 2,7 cases per year. The authors found more cases in the winter and fewer in the summer, such as Allen et al. (2010). The difference between the results of the present study and Bitencourt et al. (2013) can be explained by the choice of spatial domain: they analyzed the domain of 15°S and 45°S, 60°W and 20°W, while here much of the South Atlantic (15°S and 60°S, 75°W and 10°W) was used. Besides, the better quality of high-resolution data and direct visual examination of mslp charts employed here also influence the results (Avila 2018). It is also important to note that this study has analyzed only two years. Certainly, it brings some impact on seasonality. However, it is noteworthy that in a study on generic extratropical cyclones

Table I. **Intensity, in Bergeron, of the cases for both reanalyses and seasonal distribution in 2014.**

Cases	Intensity MERRA-2	Intensity NCEP2	Seasons
03 - 04 JAN	1,96	1,89	SUMMER
15 - 16 JAN	1,05	0,54	
25 - 26 JAN	1,21	0,96	
01 - 02 FEB	1,15	1,00	
05 - 06 FEB	1,22	1,39	
12- 13 FEB	1,41	1,09	
13 - 14 MAR	1,13	NOT IDENTIFIED	
15 - 16 MAR	1,64	1,38	
31 MAR - 01 APR	1,11	1,13	AUTUMN
12 - 13 APR	2,38	1,89	
19 - 20 MAY	1,21	1,31	
22 - 23 MAY	1,45	1,77	
04 - 05 JUN	1,37	0,83	
13 - 14 JUN	1,21	1,05	
17 - 18 JUN	2,44	0,77	
19 - 20 JUL	1,14	0,46	WINTER
07 - 08 AUG	1,70	1,36	
18 - 19 AUG	1,08	1,30	
30 - 31 AUG	1,17	0,68	
21 - 22 SEP	1,44	1,26	SPRING
24 - 25 SEP	1,37	0,93	
01 - 02 OCT	2,05	1,57	
10 - 11 OCT	1,30	1,23	
24 - 25 OCT	1,13	0,79	
30 - 31 OCT	1,17	1,18	
08 - 09 NOV	1,69	NOT IDENTIFIED	
22 - 23 NOV	1,22	0,90	
22 - 23 DEC	1,81	1,53	SUMMER

(of any intensity) on the east coast of South America, Gan & Rao (1991) also found spring as a preponderant season for systems arising south of 30ºS. In the cyclogenetic area of the La Plata River. Reboita et al. (2010), using the RegCM3 model, also found a higher frequency of generic cyclones in the spring.

As for the intensities, the impact of grid resolution seems to be remarkable. While with the finer reanalysis, 20 weak, 19 moderate, and 10 intense cases were identified, with the coarser reanalysis, 17 weak, 14 moderate, and only 2 intense cases (in the summer and autumn of 2014) were detected, which made it impossible to define a season with a higher frequency of intense explosive cyclones using this reanalysis. For MERRA-2 the most intense cases were found in summer. It is noted that in the spring – the most recurrent season of explosive cyclones for both reanalyses – there is a higher frequency

Table II. Intensity, in Bergeron, of the cases for both reanalyses and seasonal distribution in 2015.

Cases	Intensity MERRA-2	Intensity NCEP2	Seasons
15 - 16 JAN	1,85	1,53	SUMMER
19 - 20 JAN	1,54	1,33	
30 - 31 JAN	1,82	1,28	
21 - 22 MAR	0,88	1,02	AUTUMN
26 - 27 MAR	1,02	0,98	
08 - 09 MAY	1,09	1,02	
02 - 03 JUN	1,43	0,82	
15 - 16 JUN	1,90	NOT IDENTIFIED	
10 - 11 JUL	1,57	1,55	WINTER
13 - 14 JUL	1,42	1,36	
31 JUL - 01 AUG	1,85	1,45	
01 - 02 SEP	1,27	0,87	
09 - 10 SEP	1,66	1,45	
11 - 12 SEP	2,08	NOT IDENTIFIED	
16 - 17 SEP	1,48	NOT IDENTIFIED	
26 - 27 SEP	0,89	1,11	SPRING
28 - 29 SEP	1,49	1,08	
02 - 03 OCT	1,06	0,74	
08 - 09 OCT	1,00	1,04	
22 - 23 OCT	1,78	1,29	
24 - 25 OCT	1,30	1,09	
28 - 29 NOV	1,25	1,02	
09 - 10 DEC	1,43	1,05	

of moderate systems by MERRA-2 and a higher frequency of weak cases according to NCEP2 (Table III). The finer reanalysis has a higher density of grid points, enabling the identification of sea level pressure values closer to the center of the cyclone, and thus shows a higher intensity during explosive development.

Figures 1, 2, and 3 (a and c – MERRA-2; b and d – NCEP2) show the trajectories of weak, moderate, and intense cases, respectively, that occurred in 2014 and 2015, from cyclogenesis to the end of the explosive phase, distributed according to both reanalyses. Some cases have their explosive phase just at the beginning of cyclogenesis. It was noticed that the difference in spatial resolution affected the description of the systems' displacements. MERRA-2 described cyclone movements in a more smoothed way due to the higher density of grid points, refining the information in the region. On the other hand, due to the very large spacing between grid points in NCEP2, the estimates of cyclone trajectories seem to be less accurate.

Despite the variations, in general, it was noted that cyclones have been formed in the cyclogenetic regions identified in Gan & Rao (1991), near the coast of Uruguay and southern Brazil. Besides, some of these originated from an inverted trough in the surface (Piva et al. 2010), prolonged from the region leeward of the Andes. The transition between the continental low (inverted trough) and the extratropical

Table III. Numbers of events classified according to NDR for each season and each reanalysis, for the years 2014 and 2015.

	WEAK		MODERATE		INTENSE		TOTAL	
	MERRA	NCEP	MERRA	NCEP	MERRA	NCEP	MERRA	NCEP
Summer	5	3	3	5	4	1	12	9
Autumn	5	4	3	2	3	1	11	7
Winter	4	0	5	6	2	0	11	6
Spring	6	10	8	1	1	0	15	11
Total	20	17	19	14	10	2	49	33

cyclone is common in South America (Caballero et al. 2018).

A preferential displacement of the systems southeastward is noted. As explosive cyclones developed preferentially in a baroclinic zone, their displacement is mainly due to temperature advection (Bluestein 1993). This factor, combined with the eastward movement of the upper-level westerlies, contributes to the trajectories shown in figures 1, 2, and 3.

As can be seen in Figures 1 and 2, weak and moderate cyclones have originated in a wide area, therefore not presenting a characteristic formation region. On the other hand, it is common to find them with ordinary cyclogenesis over the continent, with the explosive phase starting only on the ocean, for both reanalyses.

Two cases presented a displacement to the northeast, with trajectories in dark blue and dark purple (Figure 1a-d and 2a-d), representing the cases of March 26-27 (Figure 1c) and October 24-25 (Figure 2c), respectively. Both have similar behaviors because they begin as a surface cyclone east of a transient trough at upper levels and quickly their centers are under the axis of this trough. This indicates that they reached the end of the baroclinic cycle, and should dissipate according to Simmonds & Hoskins (1978); however, the systems continued to intensify. Dias Pinto & Da Rocha (2011) analyzed the energetics and the structure of three cyclones, with one of them developing in a region of weak baroclinicity. The authors observed that the most energetic phase of the cyclone was at the beginning, in which barotropic conversion was the most important factor, transforming the kinetic energy of zonal flow into kinetic energy of disturbance through the eddy momentum fluxes. This also seems to explain the development of these two systems here identified during much of the explosive phase. Moreover, when the systems become barotropic the temperature advection does not play the same role in the trajectory as in the case of baroclinic systems, which may explain the shift northeastward.

Among the intense cases for MERRA-2 reanalysis (Figures 3a and 3c), a similarity was noted related to the region of origin of the explosive phase (between 35°S and 40°S, 40°W and 30°W) for 2015, except for one single event that occurred further west, at the end of July (shown in light red). For the year 2014, the region of origin was located further west (between 40°S and 45°S, 50°W, and 40°W) including 3 of the 5 cases. They all intensified in a baroclinic environment, with a strong horizontal temperature gradient (not shown here). In addition, two cases stood out in 2015, since they developed in the vicinity of an older cyclone. Despite being in different seasons, summer and autumn, such systems originated approximately in the same region, on the coast of Uruguay and east of extreme south of Brazil, respectively. Both presented a very similar

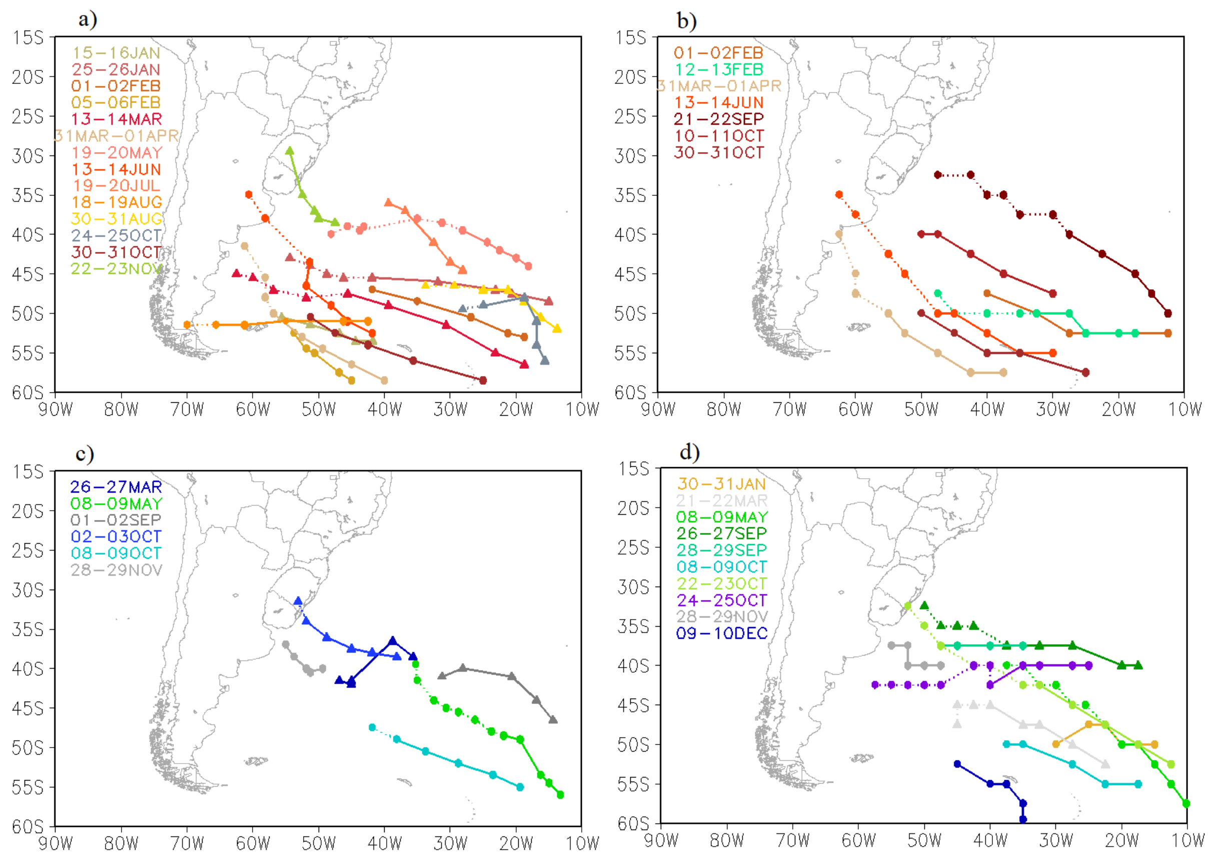

Figure 1. Trajectories of weak explosive cyclones (dashed lines – non-explosive phase; solid lines – explosive phase): a) MERRA-2 in 2014; b) NCEP2 in 2014; c) MERRA-2 in 2015; d) NCEP2 in 2015. Systems with solid circle trajectories are common cases of the two reanalyses, while those with solid triangle trajectories are cases only of the presented reanalysis.

development, distinguishing themselves only in the final position. The summer case had a shift to the southeast, while the autumn one had a shift to the south. The two cases observed using data from NCEP occurred in 2014 and presented the same direction (southeast) but originated in different regions (Figure 3b).

According to MERRA-2 data, 35 explosive cyclones that developed downstream of a preexisting upper-level trough were found (Figure 4a), and therefore are characterized as type B as stated in Petterssen & Smebye (1971). For the NCEP2 reanalysis, 28 cases of type B were observed (Figure 4b). On the other hand, with MERRA-2, 14 systems were identified in which the initial developments occurred without the presence of preexisting trough at upper levels – such trough appeared during surface cyclones development, characterizing it as type A (Figure 4a). Employing NCEP2 data, 5 cases were found as type A (Figure 4b). It is important to highlight that for some cases studied here the Petterssen & Smebye classification was not the same for the two reanalyses. This was due to one reanalysis identifying the cyclone in a different time instant from the other.

A confluence of subtropical and polar jets was detected upstream of the upper-level trough associated with the surface system was observed in 29 cases. Such upstream confluence (not shown here) is observed in the same cases

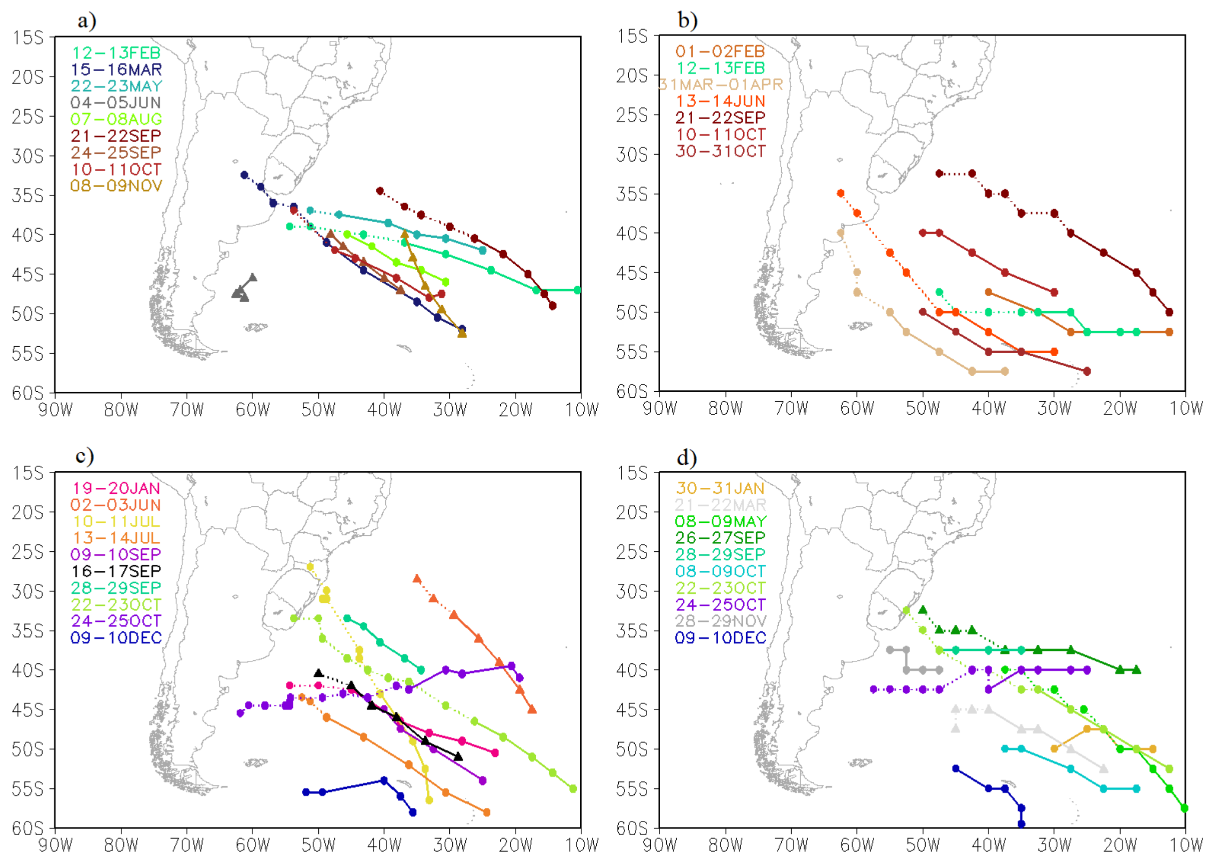

Figure 2. Trajectories of moderate explosive cyclones (dashed lines – non-explosive phase; solid lines – explosive phase): a) MERRA-2 in 2014; b) NCEP2 in 2014; c) MERRA-2 in 2015; d) NCEP2 in 2015. Systems with solid circle trajectories are common cases of the two reanalyses, while those with solid triangle trajectories are cases only of the presented reanalysis.

in the two reanalyses, as both similarly represent the jets.

Reanalyses are strongly limited by available observations that are assimilated by the respective models. In regions where observation coverage is sparse, such as Southern Hemisphere, reanalysis data are more dependent on the model and physical parametrizations when compared to the Northern Hemisphere, where observations are abundant (Hanson et al. 2004). This can produce different results between the hemispheres, emphasizing the difference between the reanalyses. Thus, high-resolution reanalyses are a more powerful tool for studies in the South Hemisphere region (Allen et al. 2010).

Composite fields

The composite fields presented in this section show the grid-centered cyclone with negative longitudes (latitudes) on the west (south) and positive on the east (north) side. These fields show very well the life cycle of extratropical cyclones for both intensities, in which baroclinicity and energy conversion become important in the development of the system, while barotropic processes are significant in maturation (Simmonds & Hoskins 1978, Randel & Stanford 1985, Holton 2004, Reboita et al. 2017a). Regardless of intensity, the negative horizontal inclination of the trough is observed in mid levels during the systems' development (Figures 5a, b, c, d, and e and 6a, b, c, d, and e).

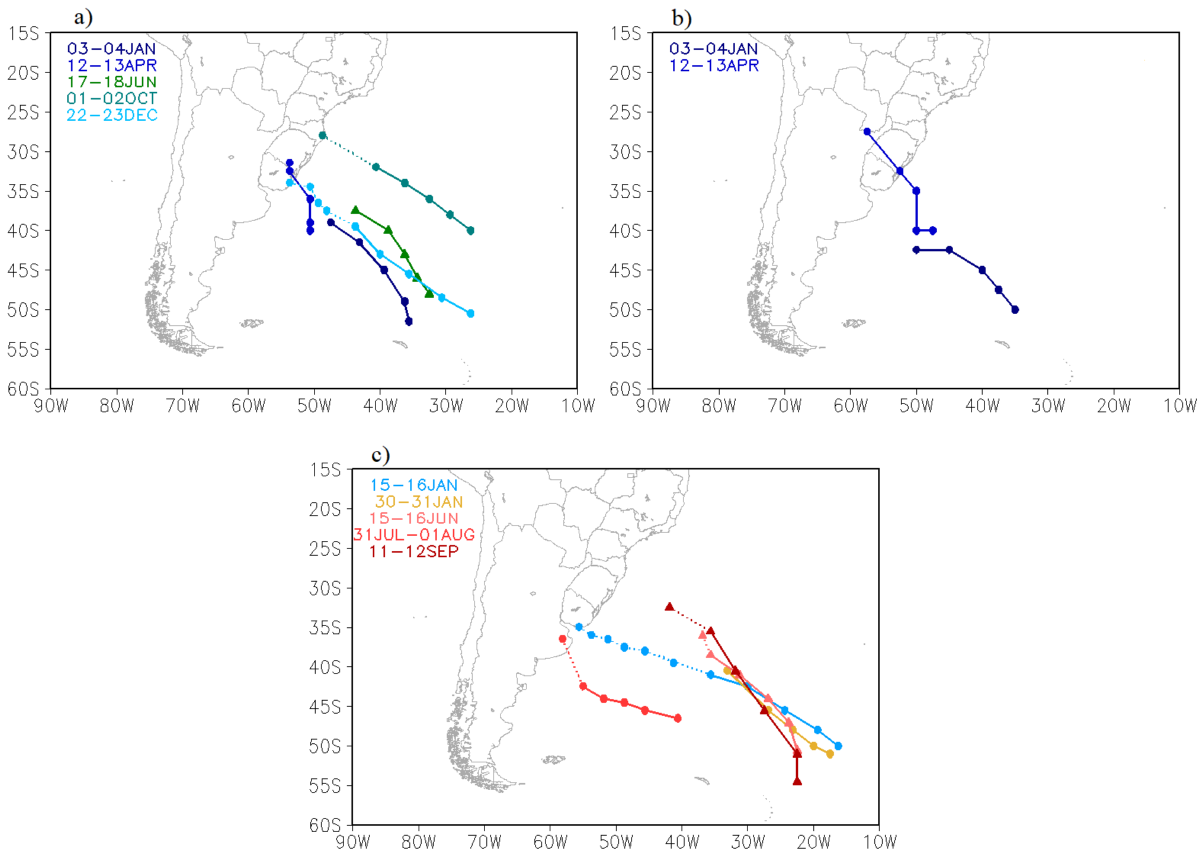

Figure 3. Trajectories of intense explosive cyclones (dashed lines – non-explosive phase; solid lines – explosive phase): a) MERRA-2 in 2014; b) NCEP2 in 2014; c) MERRA-2 in 2015. Systems with solid circle trajectories are common cases of the two reanalyses, while those with solid triangle trajectories are cases only of the presented reanalysis.

According to MacDonald (1976) and Cossetin et al. (2016), the negative slope indicates extremely severe instability, which was a consequence of the significant increase in convective activity (not shown here).

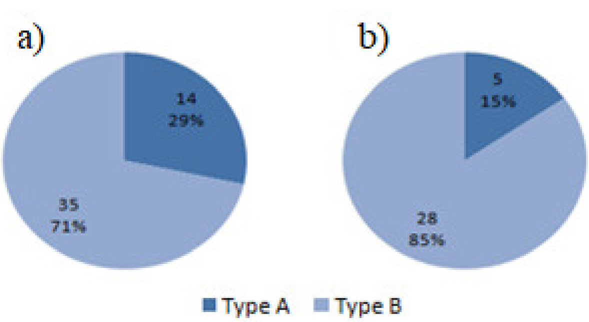

Figure 4. Classification of cyclones as type A and B for: a) MERRA-2; b) NCEP2.

At the beginning of the explosive phase, it is observed that the trough has a greater amplitude in intense cases (Figure 5) when compared to non-intense ones (Figure 6), hence indicating more intense temperature advection. Besides that, it was observed that the most intense cases have a greater geopotential height gradient. Analyzing a reference level, for example, 5600 gpm, it is detected that the most intense cases start in a thicker (warm) layer.

Wind fields show a stronger jet in intense explosive cyclones (Figures 7a, b, c, d, and e). The thermal wind balance indicates that the relationship between the temperature gradient and the vertical shear of the wind gives rise to the jet stream (Kousky & Elias 1982, Bluestein

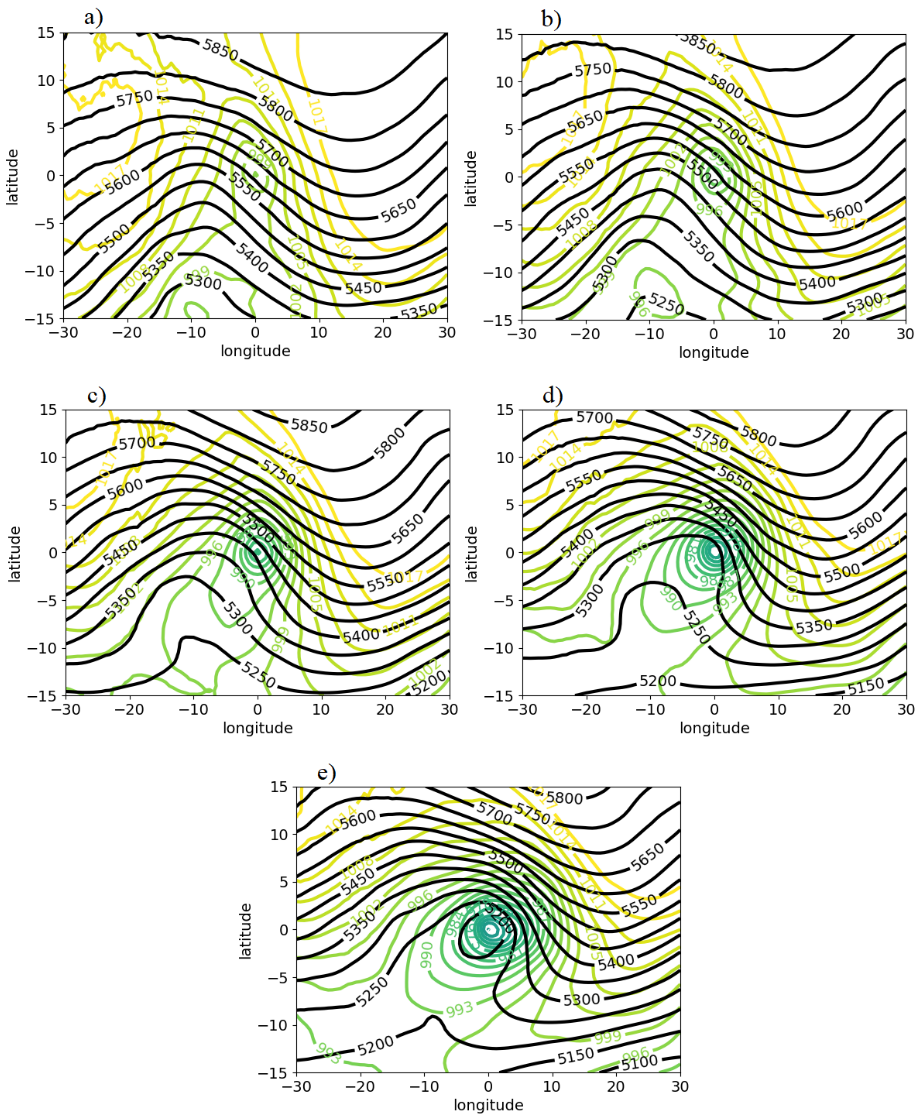

Figure 5. Composite fields of mean sea level pressure with 3 hPa intervals (colored solid lines) and geopotential height at 500 hPa with 50 gpm intervals (black solid lines) for intense cases: a) t0 (beginning of explosive phase); b) t1; c) t2; d) t3; e) t4 (end of explosive phase).

1993, Lima & Nunes 2018). Consequently, this result shows that the wind increases in intensity with the height more vigorously in the intense explosive cyclones and gives evidence that these are associated with a higher temperature gradient. Also, baroclinic systems are always associated with the wave-like pattern of the jet stream, decreasing their wavelength and leading, in some cases, to the formation of upper tropospheric cyclonic vortexes, as observed in intense cases (Bluestein 1993, Nunes 2017, Lima & Nunes 2018).

Difluent flow at upper levels was observed over the surface cyclone in 21 of the 31 cases identified by both reanalyses, mainly during the explosive phase in the exit of the jetstream. Besides highlighting this phenomenon, during the development, this feature is clearer using finer reanalysis. Sanders (1993) showed idealized patterns of flows at higher levels to ascertain the relationship of difluence in the deepening of low surface pressures. The author found that, in the scale of the disturbance and on an approximately geostrophic flow, there is a strong relationship between the intensification of the

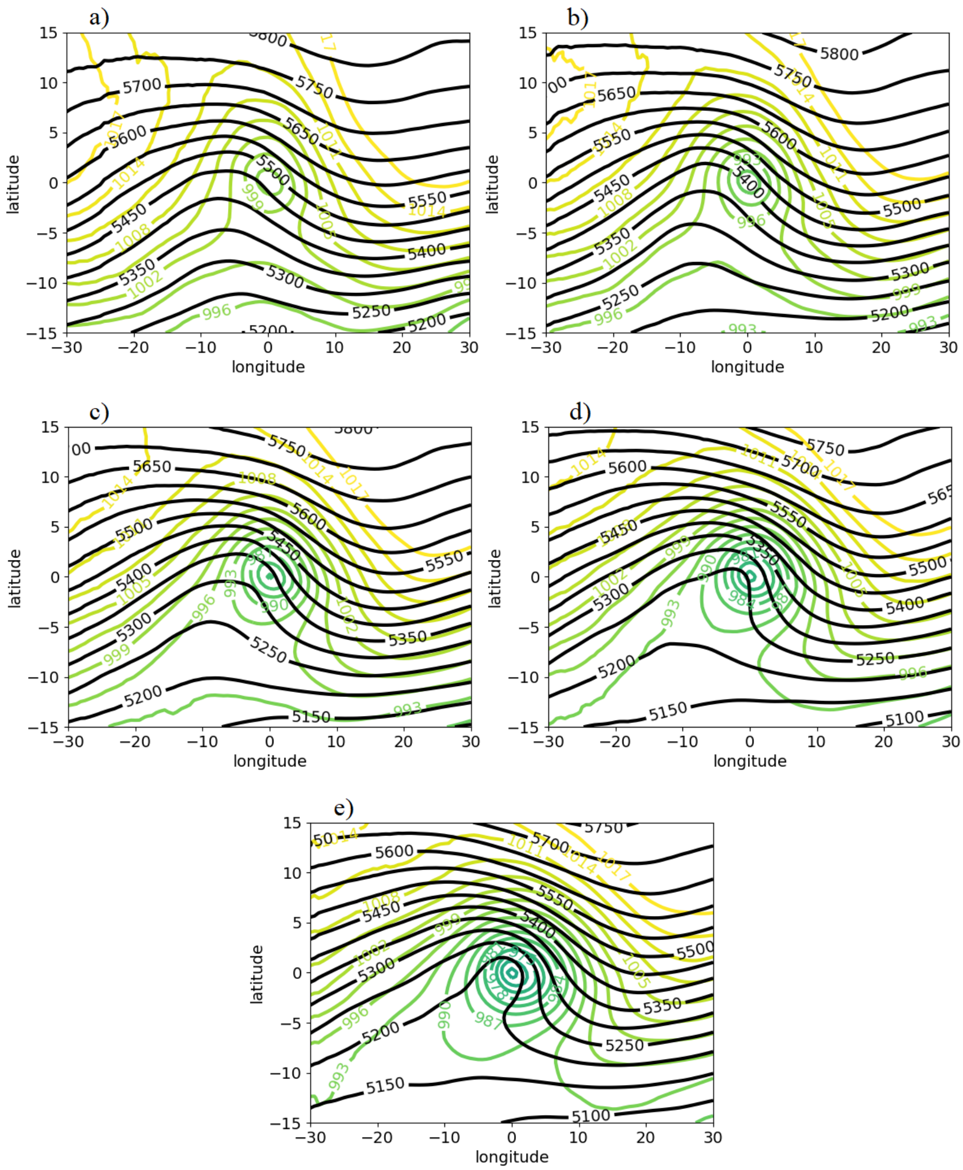

Figure 6. Composite fields of mean sea level pressure with 3 hPa intervals (colored solid lines) and geopotential height at 500 hPa with 50 gpm intervals (black solid lines) for non-intense cases: a) t0 (beginning of explosive phase); b) t1; c) t2; d) t3; e) t4 (end of explosive phase).

surface system with an upstream difluent trough, under the vorticity advection region. Thus, mass convergence at low levels is emphasized, providing deep convection, correlated with this pattern.

Concerning intensity, it was observed that the difluence at upper levels over the surface system is clearer in non-intense explosive cyclones than in intense ones (Figures 8a, b, c, d, and e). Besides, it was also diagnosed that the difluence accompanies the jetstreak exit for any type of intensity. In intense cases, the same occurs over the cyclone, up to 12 hours after the beginning of the explosive phase, while in non-intense cases up to 6 hours (Figures 7 and 8). According to Schultz et al. (1998), classic cyclones occur associated with difluent flow at higher levels; in the same way, a confluent flow at upper levels is linked with the Shapiro-Keyser type (Reboita et al. 2017b).

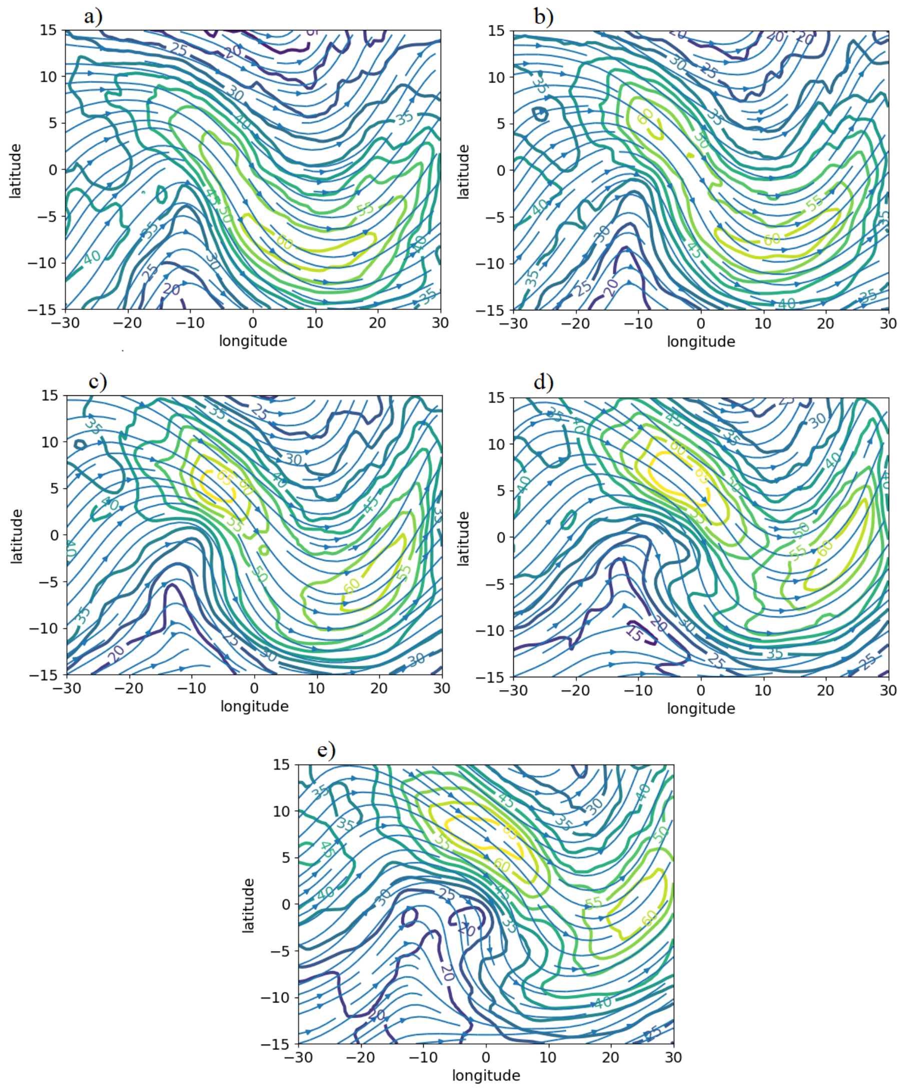

Figure 7. Composite fields of wind magnitude at 250 hPa with 5 m/s intervals (colored solid lines) and streamlines at 250 hPa (blue thin lines) for intense cases: a) t0 (beginning of explosive phase); b) t1; c) t2; d) t3; e) t4 (end of explosive phase).

CONCLUSIONS

This work presented an analysis of explosive cyclones in South Atlantic comparing MERRA-2 (higher spatial resolution) and NCEP2 (lower spatial resolution) reanalyses in 2014 and 2015. According to MERRA-2 49 cases of explosive cyclones were identified, among which 10 were intense (NDR > 1,8), while NCEP2 detected 33 cases and only 2 intense cases. A higher frequency of events in the spring was observed for both reanalyses, which disagrees with previous studies about explosive cyclones which exhibited the highest frequency in the winter. Such disagreement may lie mainly in the period extent studied. However, some similar studies, but on ordinary cyclones, indicate a higher frequency in the spring.

Among the 5 intense cases identified by the MERRA-2 reanalysis in 2015, 4 started the explosive phase in a similar region (between 35°S and 40°S, 40°W and 30°W). For the year 2014, 3 of 5 cases occurred in an equivalent area, further west (between 40°S and 45°S, 50°W and 40°W) showing a strong baroclinicity in the region.

The importance of the method used in the identification of the systems stands out: monitoring of mslp fields through the

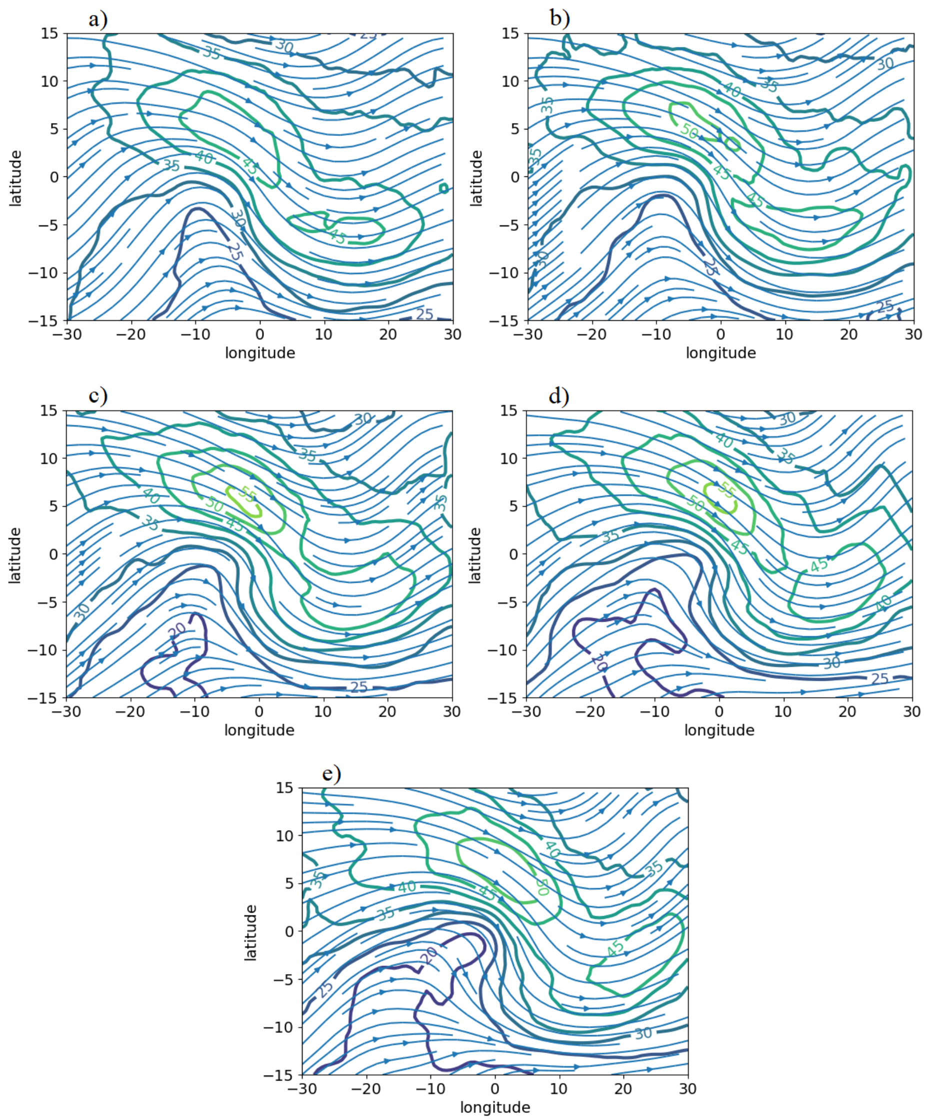

Figure 8. Composite fields of wind magnitude at 250 hPa with 5 m/s intervals (colored solid lines) and streamlines at 250 hPa (blue thin lines) for non-intense cases: a) t0 (beginning of explosive phase); b) t1; c) t2; d) t3; e) t4 (end of explosive phase).

observation of the minimum locations at each grid point, which was possible to detect a few cases where there was no closed vortex in the mslp field. In these cases, the method showed a minimum value of mslp at the grid point in the region of the figure, enabling the identification of the cyclone. Nevertheless, for good detection, a finer reanalysis with a larger amount of information is important.

The analysis of the 51 cases showed that MERRA-2 has a greater ability to distinguish type A and B systems, identifying 14 and 35, respectively. This difference is most noticeable in NCEP2 reanalysis where there were 28 type B and only 5 type A. Strictly speaking, this remarkable difference between MERRA-2 and NCEP2 is explained by distinction in spatial resolution, identifying the cyclone in an earlier or later time step, or also by the inequalities that occurred between the reanalyses to upper levels, as well as to low levels. At upper levels, the finer reanalysis detected with greater clarity and persistence difluent flows in the explosive phase around the cyclone, or over it, which indicates an important characteristic associated with instability. A confluence pattern of subtropical and polar jets upstream of the upper-level trough associated with the surface system was noted in 29 cases during the analyzed period.

The analysis of the composite fields indicated, for intense (NDR > 1,80) and non-intense (NDR ≤ 1,80) cases, a life cycle of a typical extratropical cyclone during the explosive phase. A negative horizontal tilt of the trough at 500 hPa, influenced by intense convection while the system is developing, was observed. Besides, a sharper jet in the intense explosive cyclones, indicating a superlative horizontal temperature gradient in these systems, was also noted. The difluence accompanied the exit of the jetstreak according to the explosive development for both intensities. This characteristic over the surface cyclone was more prominent in the non-intense and still presented a persistence of 6 hours, from the beginning of the explosive phase, while in the intense this characteristic was 12 hours.

Thus, this work showed that a higher spatial resolution tends to present a better choice for identification and to depict features in the development of explosive cyclones in South America. Hence, the reanalysis of MERRA-2 tends to be a better choice than NCEP2. Future work will address other types of reanalysis for longer periods.

REFERENCES

ALLEN JT, PEZZA AB & BLACK MT. 2010. Explosive Cyclogenesis: A global Climatology Comparing Multiple Reanalysis. J Climate 23(24): 6468-6484.

ATLAS R. 1987. The Role of Oceanic Fluxes and Initial Data in the Numerical Prediction of an Intense Coastal Storm. Dynam Atmos Ocean 10: 359-388.

AVILA VD. 2018. Estudo de Ciclogêneses Explosivas no Atlântico Sul. 166 f. Tese (Doutorado em Sensoriamento Remoto) – Universidade Federal do Rio Grande do Sul, Porto Alegre.

AVILA VD, NUNES AB & ALVES RCM. 2016. Análise de um Caso de Ciclogênese Explosiva Ocorrido em 03/01/2014 no Sul do Oceano Atlântico. Rev Bras Geogr Fís 9(4): 1088-1099.

BENGTSSON L, HODGES KI & HAGEMANN S. 2004. Sensitivity of Large-Scale Atmospheric Analyses to Humidity Observations and Its Impact on the Global Water Cycle and Tropical and Extratropical Weather Systems in ERA40. Tellus A 56(3): 202-217.

BITENCOURT DP, FUENTES MV & CARDOSO CS. 2013. Climatologia de Ciclones Explosivos para a Área Ciclogenética da América do Sul. Rev Bras Meteorol 28(1): 43-56.

BLUESTEIN HB. 1993. Synoptic-Dynamic Meteorology in Midlatitudes. Volume II: Observations and Theory of Weather Systems, New York: Oxford University Press, 594 p.

BOSILOVICH MGR, LUCCHESI R & SUAREZ M. 2016. MERRA-2: File Specification. GMAO Office Note, n.9 (Version 1.1), 73 p, available from: http://gmao.gsfc.nasa.gov/pubs/office_notes.

CABALLERO CB, OGASSAWARA JF, DORNELES VR & NUNES AB. 2018. Precipitação pluviométrica em Pelotas/RS: tendência, sistemas sinóticos associados e influência da ODP. Rev Bras Geogr Fís 11: 1429-1441.

CHOI W, HO CH, KIM J, KIM HS, FENG S & KANG K. 2016. A Track Patterns-Based Seasonal Prediction of Tropical Cyclone Activity over the North Atlantic. J Climate 29: 481-494.

CLAUD C & TERRAY P. 2007. Revisiting the possible Links between the Quase-Biennial Oscillation and the Indian Summer Monsoon Using NCEP R-2 and CMAP Fields. J Climate 20: 773-787.

COSSETIN F, NUNES AB & TEIXEIRA MS. 2016. Análise do Movimento Vertical sob Duas Diferentes Configurações de Altos Níveis da Troposfera. Cienc Nat 38: 484-490.

DIAS PINTO JR & DA ROCHA RP. 2011. The Energy Cycle and Structural Evolution of Cyclones over Southeastern South America in Three Case Studies. J Geophys Res 166: D14112.

GAN MA & RAO VB. 1991. Surface Cyclogenesis Over South America. Mon Weather Rev 119: 1293-1302.

GAN MA & RAO VB. 1994. The Influence of the Andes Cordillera on Transient Disturbances. Mon Weather Rev 122: 1141-1157.

GAN MA & SELUCHI ME. 2009. Ciclones e Ciclogêneses. In: Cavalcanti Ifa et al., Tempo e Clima no Brasil, São Paulo: Oficina de Textos, Cap.7, p. 110-125.

GU D, LI T, JI Z & ZHENG B. 2010. On the Phase Relations between the Western North Pacific, Indian, and Australian Monsoons. J Climate 23: 5572-5589.

GYAKUM JR ET AL. 1996. A Regional Model Intercomparison Using a Case of Explosive Oceanic Cyclogenesis. Weather Forecast 11: 521-543.

HANSON CE, PALUTIKOF JP & DAVIES TD. 2004. Objective Cyclone Climatologies of the North Atlantic – A Comparison Between the ECMWF and NCEP Reanalysis. Climate Dynam 22: 757-769.

HODGES KI, COBB A & VIDALE PL. 2017. How well are tropical cyclones represented in reanalysis datasets? J Climate 30: 5243-5264.

HODGES KI, HOSKINS BJ, BOYLE J & THORNCROFT CA. 2003. Comparison of Recent Reanalysis Datasets Using Objective Feature Tracking: Storm Tracks and Tropical Easterly Waves. Mon Weather Rev 131: 2012-1037.

HODGES KI, LEE RW & BENGTSSON LA. 2011. Comparison of Extratropical Cyclones in Recent Reanalyses ERA-Interim, NASA MERRA, NCEP CFSR, and JRA-25. J Climate 24: 4888-4906.

HOLTON JR. 2004. An Introduction to Dynamic Meteorology, 4.ed, San Diego: Elsevier, 540 p.

HOSKINS BJ & HODGES KI. 2002. New Perspectives on the Northern Hemisphere Winter Storm Tracks. J Atmos Sci 59: 1041-1061.

HOSKINS BJ & HODGES KI. 2005. A New Perspective on Southern Hemisphere Storm Tracks. J Clim 18: 4108-4129.

KALNAY E ET AL. 1996. The NCEP/NCAR 40-year Reanalysis Project. Bull Am Meterol Soc 77(3): 137-471.

KANAMITSU M, EBISUZAKI W, WOOLEN J, YANG SK, HNILO JJ, FIORINO M & POTTER GL. 2002. NCEP-DOE AMIP-II Reanalysis (R-2). Bull Am Meteorol Soc 83: 1631-1643.

KENNEDY AD, DONG X, XI B, XIE S, ZHANG Y & CHEN J. 2011. A Comparison of MERRA and NARR Reanalysis with the DOE ARM SGP Data. J Climate 24: 4541-4557.

KOUSKY VE & ELIAS M. 1982. Meteorologia Sinótica: Parte I, São José dos Campos: INPE, 118 p.

KUWANO-YOSHIDA A & ENOMOTO T. 2013. Predictability of Explosive Cyclogenesis over the Northwestern Pacific Region Using Ensemble Reanalysis. Mon Weather Rev 141: 3769-3785.

LIANG X-Z, LI L & KUNKEL K. 2004. Regional Climate Model Simulation of U.S. Precipitation during 1982-2002. Part I: Annual Cycle. J Climate 17: 3510-3529.

LIM EP & SIMMONDS I. 2002. Explosive Cyclone Development in the Southern Hemisphere and a Comparison with Northern Hemisphere Events. Mon Weather Rev 130: 2188-2209.

LIMA MV & NUNES AB. 2018. Comportamento Climático do Balanço do Vento Térmico na América do Sul de Acordo com os Eventos ENOS: Estudo Preliminar. Rev Bras Geog Fís 11(3): 728-744.

MACDONALD N. 1976. On the Apparent Relationship Between Convective Activity and the Shape of 500 mb Troughs. Mon Weather Rev 104(12): 1618-1622.

MENDES D, MOURA RG & MENDES MCD. 2009. Estudo de Caso de Ciclone Extratropical sobre a América do Sul: Sensibilidade das Análises. Rev Bras Meterol 24(4): 399-406.

MURRAY RJ & SIMMONDS I. 1991. A Numerical Scheme for Tracking Cyclone Centres from Digital Data. Part I: Development and Operation of the Scheme. Aust Meteorol Mag 39: 155-166.

NUNES AB. 2017. Case Study of Upper Tropospheric Meteorological Systems on South America: Synoptic Analysis. An Inst Geocienc 40: 70-82.

PETTERSSEN S & SMEBYE SJ. 1971. On the Development of Extratropical Cyclones. Q J Roy Meteorol Soc 97: 457-482.

PILLAR HR, JOHNSON HL, MARSHALL DP, HEIMBACH P & TAKAO S. 2018. Impacts of Atmospheric Reanalysis Uncertainly on Atlantic Overturning Estimates at 25ºN. J Climate 31: 8719-8744.

PIVA ED. 2001. Estudo de Caso sobre o Papel dos Fluxos de Calor Latente e Sensível em Superfície em Processos de Ciclogênese de Costa Leste Ocorrido na Costa da América do Sul. 162 f. Dissertação (Mestrado em Meteorologia) – Instituto Nacional de Pesquisas Espaciais, São José dos Campos. (Unpublished).

PIVA ED, GAN MA & MOSCATI MCL. 2011. The Role of Latent and Sensible Heat Fluxes in an Explosive Cyclogenesis over the South American East Coast. J Meteorol Soc Japan 89(6): 637-663.

PIVA ED, GAN MA & RAO VB. 2010. Energetics of Winter Troughs Entering South America, Mon Weather Rev 138: 1084-1103.

PIVA ED, MOSCATI MCL & GAN MA. 2008. Papel dos Fluxos de Calor Latente e Sensível em Superfície Associado a um Caso de Ciclogênese na Costa Leste da América do Sul. Rev Bras Meterol 23(n): 450-476.

RANDEL WJ & STANFORD JL. 1985. The Observed Life Cycle of a Baroclinic Instability. J Atmos Sci 42(13): 1364-1373.

REBOITA MS, DA ROCHA RP, AMBRIZZI T & SUGAHARA S. 2010. South Atlantic Ocean Cyclogenesis Climatology Simulated by Regional Climate Model (RegCM3). Climate Dynam 35: 1331-1347.

REBOITA MS, GAN MA, DA ROCHA RP & CUSTÓDIO IS. 2017a. Ciclones em Superfícies nas Latitudes Austrais: Parte I – Revisão Bibliográfica. Rev Bras Meteorol 32(2): 171-186.

REBOITA MS, GAN MA, DA ROCHA RP, CUSTÓDIO IS. 2017b. Ciclones em Superfícies nas Latitudes Austrais: Parte II Estudos de Casos. Rev Bras Meteorol 32(4): 509-542.

RIENECKER MM ET AL. 2011. MERRA: NASA's Modern-Era Retrospective Analysis for Research and Applications. J Climate 24: 3624-3648.

ROEBBER PJ. 1984. Statistical Analysis and Updated Climatology of Explosive Cyclones. Mon Weather Rev 112(8): 1577-1589.

SANDERS F. 1986. Explosive Cyclogenesis in the West-Central North Atlantic Ocean, 1981-84. Part I: Composite Structure and Mean Behavior. Mon Weather Rev 114: 1781-1794.

SANDERS F. 1993. Upper-level Geostrophic Diffluence and Deepening of Surface Lows. Weather Forecast 8: 339-344.

SANDERS F & GYAKUM JR. 1980. Synoptic-Dynamic Climatology of the "Bomb". Mon Weather Rev 108(10): 1589-1606.

SATYAMURTY P, FERREIRA CC & GAN MA. 1990. Cyclonic Vortices over South America. Tellus A 42(1): 194-201.

SCHULTZ DM ET AL. 2018. Extratropical Cyclones: A Century of Research on Meteorology's Centerpiece. Meteorol Monogr 59: 16.

SCHULTZ DM, KEYSER D & BOSART LF. 1998. The Effect of Large Scale Flow on Low-Level Frontal Structure and Evolution in Midlatitude Cyclones. Mon Weather Rev 126(7): 1767-1791.

SELUCHI ME & SAULO AC. 1988. Possible Mechanisms Yielding an Explosive Coastal Cyclogenesis over South America: Experiments Using a Limited Area Model. Austr Meteorol Mag 47(4): 309-320.

SIMMONDS AJ & HOSKINS BJ. 1978. The Life Cycles of Some Nonlinear Baroclinic Waves. J Atmos Sci 35: 414-432.

SINCLAIR MR. 1994. An Objective Cyclone Climatology for the Southern Hemisphere. Mon Weather Rev 122: 2239-2256.

SINCLAIR MR. 1995. A Climatology of Cyclogenesis for the Southern Hemisphere. Mon Weather Rev 123: 1601-1619.

TRIGO IF. 2006. Climatology and Interannual Variability of Storm-Tracks in the Euro-Atlantic Sector: A Comparison between ERA-40 and NCEP/NCAR Reanalysis. Climate Dynam 26: 127-143.

VERA CS, VIGLIAROLO PK & BERBERY EH. 2002. Cold Season Synoptic-Scale Waves over Subtropical South America. Mon Weather Rev 130: 684-699.

WASH CH, HALE RA, DOBOS PH & WRIGHT EJ. 1992. Study of Explosive and Nonexplosive Cyclogenesis during FGGE. Mon Weather Rev 120: 40-51.

YAO Y, LIANG S, QIN Q & WANG K. 2010. Monitoring Drought over the Conterminous United States Using MODIS and NCEP Reanalysis-2 Data, J Apll Meteorol Clim 49: 1665-1680.

How to cite

ANDRADE HN, NUNES AB & TEIXEIRA MS. 2022. South Atlantic Explosive Cyclones in 2014-2015: Study Employing NCEP2 and MERRA-2 Reanalyses. An Acad Bras Cienc 94: e20200797. DOI 10.1590/0001-3765202220200797.

Manuscript received on May 27, 2020;
accepted for publication on May 15, 2021

HUGO N. ANDRADE[1]
https://orcid.org/0000-0002-0698-2100

ANDRÉ B. NUNES[2]
https://orcid.org/0000-0002-4881-5810

MATEUS S. TEIXEIRA[2]
https://orcid.org/0000-0001-5712-9938

[1]Programa de Pós-Graduação em Sensoriamento Remoto - PPGSR, Universidade Federal do Rio Grande do Sul, Av. Bento Gonçalves, 9500, Agronomia, 91501-970 Porto Alegre, RS, Brazil

[2]Programa de Pós-Graduação em Meteorologia, Universidade Federal de Pelotas, Campus Universitário, s/n, Capão do Leão, 96010-610 Pelotas, RS, Brazil

Correspondence to: **Hugo Nunes Andrade**
E-mail: hugonandrade@hotmail.com

Author contributions

Conceptualization: HNA and ABN.
Methodology: HNA, ABN and MST.
Data curation: HNA and MST.
Original draft preparation: HNA.
Formal analysis: HNA and ABN.
Reviewing and editing: HNA, ABN and MST.